ELLIS HORWOOD SERIES IN MECHANICAL ENGINEERING

Series Editor: J. M. ALEXANDER, formerly Stocker Visiting Professor of Engineering and Technology, Ohio University, Athens, USA, and Professor of Applied Mechanics, Imperial College of Science and Technology, University of London

The series has two objectives: of satisfying the requirements of postgraduate and mid-career engineers, and of providing clear and modern texts for more basic undergraduate topics. It is also the intention to include English translations of outstanding texts from other languages, introducing works of international merit. Ideas for enlarging the series are always welcomed.

lexander, J.M.
lexander, J.M., Brewer, R.C. & Rowe, G.
lexander, J.M., Brewer, R.C. & Rowe, G.
lkins A.G. & Mai, Y.W.
ards, C.F.
ards, C.F.
ards, C.F.
ards, C.F.
sant, C.B. & Lui, C.W.K.
rkowski, J. and Szymanski, A.
rkowski, J. and Szymanski, A.
ook, R. and Howard, I.C.
meron, A.
llar, A.R. & Simpson, A.
okson, R.A. & El-Zafrany, A.
okson, R.A. & El-Zafrany, A.
ig, Q.L. & Davies, B.J.
munds, H.G.
iner, D.N.
iner, R.T.
d, Sir Hugh, FRS, & Alexander, J.M.
lagher, C.C. & Knight, W.A.
iar, R.
iman, B.E., Launder, A.D. & Reece, G.
iasekera, J.S.
ldad, S.D. & Watson, N.
ldad, S.D. & Watson, N.
ldad, S.D.
it, S.E.
s, B.M. & Ahmad, S.
s, B.M. & Shrive, N.G.
ison, W. & Mellor, P.B.
isz, A.Z. and Opoczky, L.
ber, M.
ber, M. & Breitkopf, P.

h, D.J. & Turner, B.T.
ins, J.D.
in, S.
baek, J.C.
loy, D. & Martin, H.R.
zka, A.
y, P.L.B.
ek, K. and Niziol, J.
iski, S.
is, J.M.
on, J.D.
irds, T.H.
C.T.F.
C.T.F.
C.T.F.
C.T.F.
C.T.F.
D. N.
owski, T.
uk, A.
in, K.
icki, J.
inski, W. & Szlagowski, J.
, M.W.
aw, A.C.
ns, J.G.
ns, J.G.

Strength of Materials: Vol. 1: Fundamentals; Vol. 2: Applications
Manufacturing Technology Volume 1: Engineering Materials
Manufacturing Technology Volume 2: Engineering Processes
Elastic and Plastic Fracture
Vibration Analysis and Control System Dynamics
Structural Vibration Analysis
Noise Control
Vibrations and Control Systems
Computer-aided Design and Manufacture, 3rd Edition
Technology of Abrasives and Abrasive Tools
Uses of Abrasives and Abrasive Tools
Introductory Fracture Mechanics
Basic Lubrication Theory, 3rd Edition
Matrices and Engineering Dynamics
Finite Element Techniques for Engineering Analysis
Techniques of the Boundary Element Method
Surface Engineering Geometry for Computer-aided Design and Manufacture
Mechanical Foundations of Engineering Science
Engineering Stress Analysis
Engineering Elasticity
Advanced Mechanics of Materials, 2nd Edition
Group Technology Production Methods in Manufacture
Elastohydrodynamics
Computer-aided Engineering: Heat Transfer and Fluid Flow
CAD/CAM of Dies
Principles and Performance in Diesel Engineering
Design and Applications in Diesel Engineering
Advanced Diesel Engineering and Operation
Nuclear Physics for Engineers and Scientists
Techniques of Finite Elements
Finite Element Primer
Engineering Plasticity
Mechanical Activation of Silicates by Grinding
Incremental Finite Element Modelling in Non-linear Solid Mechanics
Finite Element Methods in Structural Engineering:
Turbo Pascal Programs for Microcomputers
Engineering Design for Profit
Engineering Thermodynamics
Materials Grinding: Theory and Applications of Mechining with Abrasives
Dynamics in Engineering
Control of Fluid Power: Analysis and Design, 2nd (Revised) Edition
Multicriterion Optimisation in Engineering
The Mechanics of Machining
Random Vibration of Mechanical Systems
Bulk Containers: Design and Engineering of Surfaces and Shapes
Dynamics of Mechanical Systems, 2nd Edition
Applied Elasticity
Energy Methods in Vibration Analysis
Computational Methods in Structural and Continuum Mechanics
Finite Element Programs for Axisymmetric Problems in Engineering
Finite Element Methods in Structural Mechanics
Applied Stress Analysis
Advanced Applied Stress Analysis
Applied Fluid Mechanics
Moving Heat Sources in Thermoelasticity
Mechanics and Plasticity of Structures
Engineering Design for Performance
Stress Measurement by Photoelastic Coating
Plastic Design of Complex Shape Structured Elements
Robots and Telechirs
Mechanical Vibrations with Applications
Fracture Mechanics of Polymers
Stress Analysis of Polymers 2nd (Revised) Edition

GRINDING TECHNOLOGY

Theory and Applications of Machining with Abrasives

S. MALKIN, B.S., M.S., Sc.D.
Professor of Mechanical Engineering, University of Massachusetts

1989

ELLIS HORWOOD LIMITED
Publishers · Chichester

Halsted Press: a division of
JOHN WILEY & SONS
New York · Chichester · Brisbane · Toronto

2

Grinding wheels: composition and properties

2.1 INTRODUCTION

Grinding wheels and abrasive segments fall under the general category of 'bonded abrasive tools'. Such tools consist of hard abrasive grains or grits, which do the cutting, held in a weaker bonding matrix. Depending on the particular type of bond, the space between the abrasive particles may only be partially filled — leaving gaps and porosity — or completely filled with binder. Aside from abrasive and bond material, fillers and grinding-aid materials may also be added. The properties and performance of bonded abrasive tools depend on the type of abrasive grain material, the size of the grit, the bond material, the properties of abrasive and bond, and the porosity.

Grinding wheels are made from many types of grit in a wide range of sizes, in conjunction with many bond materials and compositions. 'Conventional' wheels in common use contain either aluminum oxide or silicon carbide abrasive with vitrified or resinoid bonds. 'Superabrasive' wheels with diamond and cubic boron nitride (CBN) abrasives are produced with vitrified, resin, and metal bonds. Whereas conventional abrasive wheels usually comprise the entire bonded abrasive structure throughout, the abrasive–composite on superabrasive wheels is limited to a thin rim or layer on a plastic or metal hub in order to reduce the amount of costly diamond and CBN which is needed. The different types of grinding wheels, together with the requirements of a wide variety of wheel shapes and sizes to fit all the diverse grinding machines and jobs to be done, lead to an almost endless diversity of grinding wheels. A 'full line' grinding wheel company may produce tens of thousands of nominally different products to satisfy its customers' requirements.

In this chapter, the composition and properties of grinding wheels will be generally considered, as a basis for understanding the grinding process and wheel selection. The discussion will encompass wheel composition and its specification, abrasive grain materials, bond materials, and wheel testing.

2.2 GRINDING WHEEL SPECIFICATION: CONVENTIONAL ABRASIVES

As a first approach to the subject of wheel composition, it is convenient to refer to the standard marking systems for specifying conventional grinding wheels. The Wheel Specification defines the following parameters:

(1) the type of abrasive in the wheel;
(2) the abrasive grain size;
(3) the wheel's hardness;
(4) the wheel's structure;
(5) the bond type;
(6) any other maker's identification codes.

The standard marking system used in North America for conventional abrasive wheels containing aluminum oxide and silicon carbide abrasive is presented in Fig. 2.1 [1]. The same or similar systems are common elsewhere in the world. The

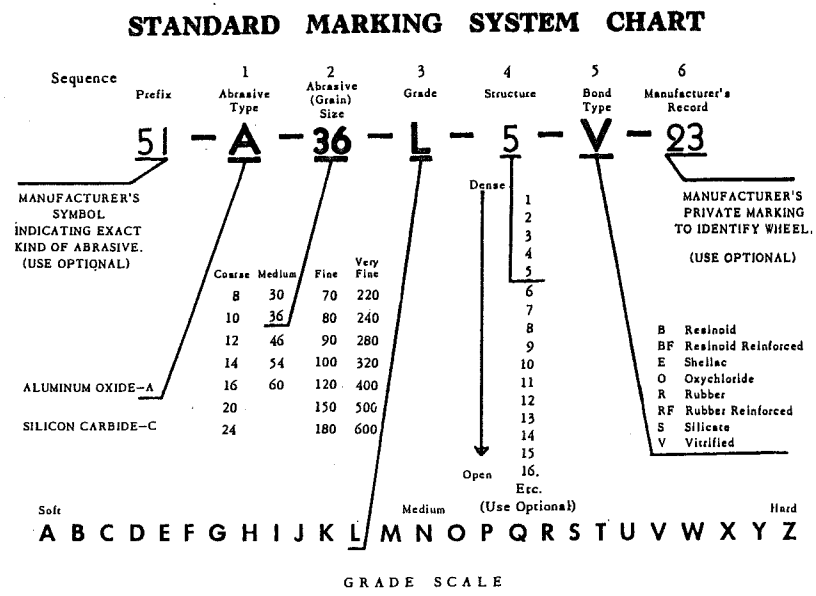

Fig. 2.1 — Standard marking system for aluminum oxide and silicon [1].

symbol A or C indicates whether the abrasive material is Aluminum oxide or silicon Carbide. In fact, there are many types of abrasive based on synthetic aluminum oxide plus two common types of silicon carbide with different chemical compositions and structural characteristics which, in turn, affect their physical and mechanical properties (section 2.4). A manufacturer's prefix (in the form of a letter or number) usually

appears to the left of the abrasive letter to indicate the particular type of alumina or silicon carbide used.

The symbol to the right of the abrasive grain type indicates the abrasive grain size, by a grit number which is related to the mesh number (specified as wires per linear inch) of the screen used to sort the grains. A larger number indicates a smaller grain size. Sieving (screening) is generally used for sizing of conventional abrasive grains coarser than 240 grit size, and a sedimentation method is used with finer grits (microgrits) [2,3]. The sieving method consists of passing abrasive grains through a stack of standard sieves from the coarser aperture sieves first through progressively finer meshes, i.e. the mesh number increases down the stack. Nominally, the aperture size decreases by a factor of $\sqrt{2}$ between adjacent sieves in a stack of standard sieves.

A standard grit number is defined in terms of grain sizes corresponding to five such sieves. For example, grit number 46 involves grains caught on sieves number 30, 40, 45, 50 and 60 using a standard sample size and sieve-shaking procedure. The specification requires 0% retention on the #30 sieve (i.e. no grains larger than 595 μm), not less than 70% passing the 'control' sieve #40 (not more than 30% in the size range 595–420 μm), not less than 40% retention on #45 (size range 420–354 μm), not less than 65% retention on #45 and #50 combined (not less than 65% in the size range 420–297 μm), and not more than 3% passing #60 (at least 97% in the size range 595–250 μm).

Since each nominal grit size includes a range of abrasive particle sizes, the grit dimension corresponding to a particular grit number might be characterized by an average value. However, the grit dimension d_g is often quoted in a simpler way either as equal to the aperture opening of the control sieve, or alternatively according to the relationship.

$$d_g \text{ (inches)} = 0.6M^{-1} \tag{2.1}$$

or equivalently

$$d_g \text{ (mm)} = 15.2M^{-1} \tag{2.2}$$

which approximates the grit dimension d_g as 60% of the average spacing between adjacent wires in a sieve whose mesh number equals the grit number M. The abrasive grain dimensions corresponding to both of these methods are plotted in Fig. 2.2 as a function of grit number. When based upon the control sieve opening, the grain dimension can be approximated by

$$d_g \text{ (mm)} = 28M^{-1.1} \tag{2.3}$$

Also included in Fig. 2.2 are results obtained for the average grain dimension obtained by sieving samples of an aluminum oxide abrasive of different grit numbers, with the dimension for the weight percentage retained on each sieve assigned as the average of that sieve opening and of the next coarser one [4]. This latter result can be approximated by

$$d_g \text{ (mm)} = 68M^{-1.4} \tag{2.4}$$

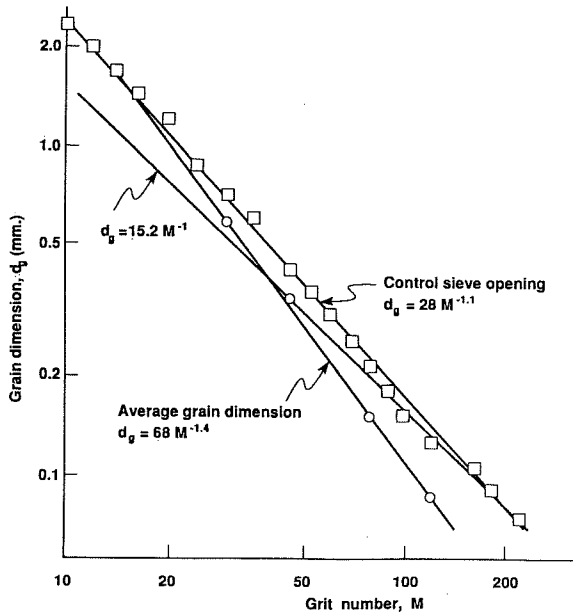

Fig. 2.2 — Grain dimension versus grit-number relationships based upon sieve wire spacing, control sieve opening, and average grain dimension.

Although this equation is strictly applicable only to the particular type of grit tested, it probably is a more precise indication of the actual grit dimension than either of the other two relationships. The three relationships in Fig. 2.2 may appear to be rather similar, but their differences can lead to significant discrepancies in calculations related to grain packing in bulk or within a grinding wheel.

Although not indicated in Fig. 2.1, some wheel manufacturers sometimes add a single digit after the grit number to indicate whether the wheel contains a mixture of grit sizes. The number 1 after the grit number usually indicates that the wheel contains abrasive grains only of the indicated grit number, whereas a different number would designate a particular mixture of grit sizes. Using a wider range of grit sizes facilitates wheel manufacture, insofar as it makes it easier to pack the abrasive grains more tightly together in molding the wheel. The blending of two or three adjacent grit sizes is probably a common practice in wheel manufacture, even though it may not be explicitly indicated in the wheel specification.

Continuing on with the wheel marking system in Fig. 2.1, the letter following the grit number signifies the wheel grade or hardness. The wheel grade provides a general indication of wheel strength and the degree to which abrasive grains are tightly held by the binder, as will be seen in sections 2.7 and 2.8. One method of establishing the wheel grade is on the basis of porosity, regardless of the relative amounts of abrasive and binder. According to one common scale, the hardest grade

Z represents 2% porosity, Y 4%, X 6%, and so on [5]. For a given grain content, a harder wheel would thus have more binder and less porosity. Hardness scales based upon porosity are not universal, and the actual porosity or effective wheel hardness for the same letter grade will vary from one manufacturer to another.

The structure number in the wheel marking (Fig. 2.1) indicates the volumetric concentration of abrasive grain in the wheel, a higher number indicating less abrasive or a more open wheel. One commonly used structure scale appears to be based upon the empirical relationship

$$V_g(\%) = 2(32-S) \qquad (2.5)$$

for volume percentage V_g of grain as a function of structure number S, which means that each structure number increment corresponds to reduction by 2% in the grain content. An upper limit on the grain concentration (lower limit on structure number) is imposed by packing limitations which refers back to the grain size and its distribution. Abrasives of a given size and shape are characterized by a limiting natural packing density which can be reached by shaking and application of moderate pressures low enough so as not to cause grain crushing. Higher limiting packing densities are obtained with coarser and more equiaxed (blocky) shaped grains than with finer and less symmetrical (weaker) shapes, and the degree of natural packing (bulk density) may be used as a rather simple but effective measure of grain shape. Maximum volumetric packing densities generally range from about 40 to 60%, although somewhat higher values are obtained with broader size distributions. At the other extreme, a lower volumetric packing density limit is imposed, at least with vitrified wheels, by the need to maintain some mutual grain contact so as to minimize shrinkage and distortion during the vitrification process of wheel manufacture.

The bond material is indicated by a letter, which may be followed by an additional notation to indicate a particular formulation. Most conventional abrasive wheels are made with vitreous- and resinoid-based bonds. The derivation of 'V' for Vitrified bond is obvious. Rubber-based bonds were once very common and have retained the designation 'R', while Resinoid bonds, first based on Bakelite, the original synthetic thermosetting plastic, have adopted 'B'. Shellac was formerly referred to as an Elastic bond, hence the designation 'E' for Shellac bonds. Silicate, 'S', and oxychloride, 'O', bonds are now almost extinct.

2.3 GRINDING WHEEL SPECIFICATION: SUPERABRASIVES

Wheels containing superabrasives — diamond or cubic boron nitride (CBN) — use a somewhat different wheel specification system which is illustrated in Fig. 2.3 [1]. The letter indicating abrasive type for diamond (D) or cubic boron nitride (B) is usually preceded by a symbol to identify a particular abrasive material. The bond material — resin, vitrified, or metal — is also indicated by a letter, often followed by an additional manufacturer's notation to identify a particular formulation. Most superabrasive wheels have either resin or metal bonds, although vitrified bonds are also beginning to be used to a significant extent for CBN wheels. As the abrasive grain is expensive, only a relatively shallow section of the active area of the wheel surface

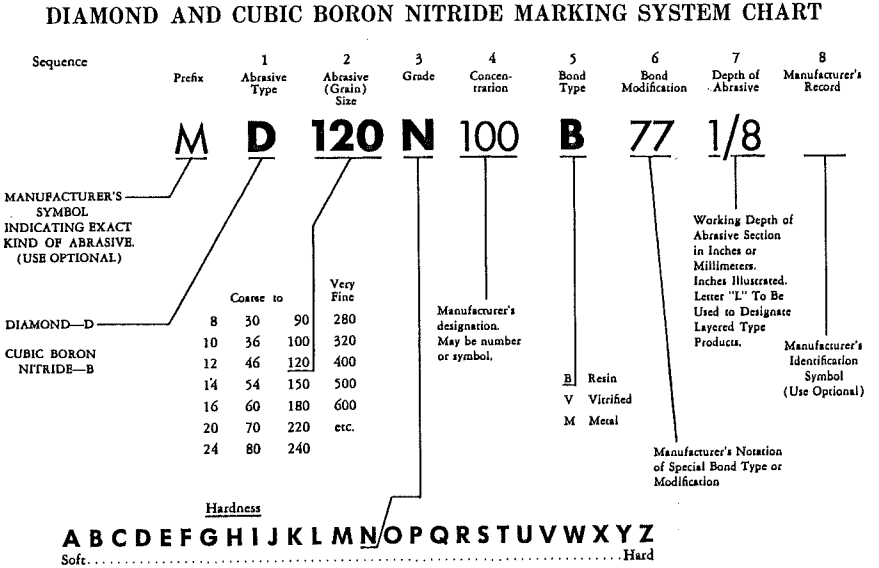

Fig. 2.3 — Standard marking system for diamond and cubic boron nitride grinding wheels and other bonded abrasives [1].

actually consists of bonded abrasive, which is attached to a metal or plastic hub. The depth of the abrasive section is indicated in the wheel marking (Fig. 2.3). Less expensive metal-bonded wheels containing less abrasive are produced by electroplating a layer of superabrasive grit onto a form or hub. In this case, the manufacturer usually specifies only the abrasive type and grit size.

Superabrasive grain sizes may be specified by grit numbers as with conventional abrasives, but the corresponding standard for checking the size of diamond grains is somewhat different and utilizes a two-number designation (see Table 2.1) [6]. The first number is generally considered to represent the sieve through which most of the grain would pass, and the second number the sieve which would retain most of the grain, although this is only approximately true. The number in the corresponding FEPA (Federation Européenne des Fabricants de Produits Abrasifs) designation in Table 2.1, which is used by many European superabrasive wheel suppliers, indicates the approximate grain dimension d_g in microns. This dimension and the second number in the grit-size designation can be shown to very nearly follow Eq. (2.2) in the size range from 40/50 down to 325/400. Superabrasive grits finer than 325/400 (powders) are checked by other methods [7].

The letter grade in the wheel marking (Fig. 2.3) provides a relative indication of the strength or hardness of the bond, as with conventional abrasives. However, resin- and metal-bonded wheels are produced with virtually no porosity, and the effective grade is obtained by changing the bond formulation (section 2.6). With

Table 2.1 — Grit-size designation for diamond and cubic boron nitride [6]

USA grit size	FEPA designation
16/18	D1181
18/20	D1001
20/30	D852
30/40	D602
40/50	D427
50/60	D301
60/80	D252
80/100	D181
100/120	D151
120/140	D126
140/170	D107
170/200	D91
200/230	D76
230/270	D64
270/325	D54
325/400	D46

resin-bonded wheels, for example, this could involve the addition of fillers in place of porosity.

Following the grade (Fig. 2.3) is the concentration number, which indicates the amount of abrasive contained in the wheel, although this is sometimes given as the related volume percentage in some systems. The concentration number is based upon a proportional scale with a value of 100 corresponding to an abrasive content of 4.4 carats/cm^3. This scale was originally developed for diamond wheels for which the concentration number divided by four equals the volumetric percentage of grit (e.g. 100 concentration is 25% by volume). The corresponding volumetric concentration for CBN is nearly the same (24%), as the density of CBN is very nearly equal to that of diamond. Typical concentrations for metal- and resin-bonded superabrasive wheels range from 50 to 150 (12.5 to 37.5 volume % for diamond). As with conventional abrasive wheels, vitrified superabrasive wheels would require higher concentrations, thereby making such wheels more costly. Less expensive vitrified CBN wheels are produced which contain a mixture of CBN and aluminum oxide abrasives.

2.4 CONVENTIONAL ABRASIVE MATERIALS

Abrasive grains, the cutting tools of the grinding process, are naturally occurring or synthetic materials which are generally much harder than the materials which they

cut. Natural abrasives include aluminum oxide (natural corondum and emery), garnet, and diamond. Technological advances in the abrasives industry have been mainly in the development of synthetic (man-made) abrasives, as discussed in Chapter 1. Some physical properties of the most important abrasive materials are summarized in Table 2.2. Conventional abrasives (aluminum oxide and silicon

Table 2.2 — Some properties of abrasive materials

	Material			
	Aluminum oxide (Al_2O_3)	Silicon carbide (SiC)	Cubic boron nitride (BN)	Diamond (C)
Crystal structure	Hexagonal	Hexagonal	Cubic	Cubic
Density (g/cm^3)	3.98	3.22	3.48	3.52
Melting point (°C)	2040	~2830	~3200 at 105 kbar (triple point)	~3700 at 130 kbar (triple point)
Knoop hardness† (kg/mm^2)	2100	2400	4700	8000

† Approximate value — depends on crystal orientation and purity.

carbide) will be considered in this section, and superabrasives (diamond and cubic boron nitride) in the following one.

Virtually all conventional abrasives in use today for grinding wheels are synthetic materials based upon either aluminum oxide (Al_2O_3) or silicon carbide (SiC). The hard aluminum oxide phase is α-alumina, having an hexagonal crystal structure like that of natural aluminum oxide abrasives (emery and corundum) which exist in various states of purity and degrees of crystallization. In addition to Al_2O_3, synthetic aluminum oxides contain various amounts of other metallic oxides either intentionally added or as impurities. Silicon carbide occurs in various polytypes, which can be generally classified as α-types having hexagonal or rhombohedral crystallographic structures and a β-type which is cubic. Silicon carbide abrasive materials consist primarily of α-SiC [8]. Several varieties of aluminum oxide abrasive, and a limited number of silicon carbide types, are in common use, each having a distinctive chemical composition and set of structural characteristics which affect the granular properties and grinding behavior and so make it useful for specific tasks.

Classically, the prime requirement of an abrasive is that it be harder than the material it is to abrade. The hardness of an abrasive is generally defined in terms of its static indentation hardness as determined by a Knoop hardness test. Another important abrasive property is its dynamic strength or toughness. High toughness

implies that an abrasive grain is less likely to fracture or fragment each time it engages or impacts the workpiece. On the other hand, a more friable (less tough) abrasive should regenerate sharp cutting edges (self-sharpen) as the grain dulls by attrition during use.

The comparative friability of conventional abrasives is usually evaluated by a standard comminution test wherein a sample of relatively coarse (#12 grit) material is ball milled under prescribed conditions [9]. The 'friability index' of the abrasive, indicating the degree of fragmentation caused, is defined as the percentage of milled material passing through a #16-mesh sieve, although this defines the value for only one grain size. Variants of this comminution method can be used in a more generalized way to determine the relative friability of different grain sizes of the same abrasive or of different abrasives [10]. In general, finer grits of the same material are less friable, which is to be expected since they are usually produced by crushing of coarser material. Friability of abrasive grains can also be evaluated using a single-blow impact test [11].

Hardness and friability data are given in Table 2.3 for many of the common types

Table 2.3 — Hardness and friability index for aluminum oxide and silicon carbide abrasives (12 grit number) [10]

Grain type	Knoop hardness (kg/mm^2)	Friability index
Aluminum oxide		
Modified (3% Cr)	2260	65.0
White	2120	56.6
Monocrystalline	2280	47.7
Regular	2040	35.6
Microcrystalline	1950	10.9
10% ZrO_2	1960	10.9
40% ZrO_2	1460	7.9
Sintered	1370	6.5
Silicon carbide		
Green	2840	62.5
Black	2680	57.2

of aluminum oxide and silicon carbide abrasives [11,12]. Harder abrasive grains are generally more friable, which can also be seen in Fig. 2.4 where the friability index is plotted versus hardness. Silicon carbide abrasives are harder than aluminum oxide, and also tend to fall towards the upper end of the friability range. Harder and more friable abrasives are generally applied to precision-grinding operations. Tougher abrasives of larger sizes are more suitable for heavy-duty grinding.

For aluminum oxide abrasives, observed differences in properties arise from

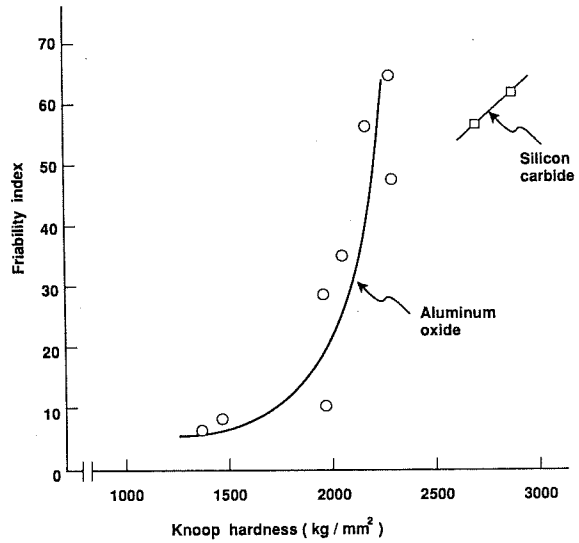

Fig. 2.4 — Friability index versus hardness for aluminum oxide and silicon carbide abrasives. Data are given in Table 2.3.

differences in chemical composition and structural characteristics associated with the manufacturing process. Starting with bauxite as the main raw material, most aluminum oxide abrasives are made by three different methods. Bauxite dehydrated by calcination may be fused directly with coke and iron in an electric furnace, it may be first processed to form purified Bayer process alumina which is then fused, or it may be sintered after pressing.

Regular or brown aluminum oxide (Table 2.3) can be produced by the first of these methods, by fusing calcined bauxite with a small amount of coke and iron. The brownish product contains about 2.7% titanium oxide retained from the bauxite, possibly as a dispersed softer β-$Al_2O_3 \cdot TiO_2$ phase, which may be responsible for the material's lower hardness and friability (higher toughness) relative to the purer white and monocrystalline varieties. The grains tend to be irregularly shaped with featureless surfaces, although second-phase inclusions can be seen with coarser-size grits [13]. This semi-friable abrasive is applied to a wide range of operations from heavy-duty grinding to roughing and semi-finishing. A tougher variation of this material referred to as microcrystalline aluminum oxide (Table 2.3), produced by more rapid cooling in smaller ingots to obtain a much finer crystal size, is used mainly for heavy-duty grinding.

Monocrystalline aluminum oxide can be produced by a similar fusion process but with the addition of iron sulfide and alkaline compounds to sweep out the titania with the other oxides. The resulting ingot consists of alumina grains in a decomposable sulfide matrix and is crushed and treated with water to release the abrasive grit. This

material is much purer than the brown product, containing only minor amounts of oxide impurities, and has the great advantage that the grains are produced by a method that does not expose them to high crushing forces before they are used in a wheel. Scanning electron microscope (SEM) observations of monocrystalline aluminum oxide reveal stepwise facets which could act as sharp cutting points [13]. This abrasive material is used mainly for finish-grinding operations.

White and modified aluminum oxide abrasives (Table 2.3) are produced by the fusion of pre-purified Bayer process alumina in the Hall–Heroult electric arc furnace. The white grades of alumina are nearly 100% Al_2O_3 and modified aluminas are produced by adding small amounts of soluble metal oxides which go into solid solution and may enhance the material's hardness and normally increase its toughness appreciably. White aluminum oxide grains have sharp fracture facets, similar to those observed on monocrystalline grains. Such facets are not observed on modified (chrome and vanadium oxide) abrasives [13].

Bayer process alumina contains small amounts of sodium oxide, and both white and modified aluminum oxide abrasives can contain up to 1% residual Na_2O. Its presence can leave voids in the final abrasive, from gassing due to removal of some of the original oxide present, and it produces so-called β-Al_2O_3 (actually a compound approximating to the formula $Na_2O{\cdot}11Al_2O_3$) in the grains, which is very soft and must be destroyed by heating to temperatures greater than 1260°C during the firing of the final abrasive tool or wheel. These abrasives are used for finish-grinding operations.

Sintered aluminum oxide is manufactured in a completely different way by pressing or extrusion of a fine (1–5 μm) paste of calcined bauxite, granulating or chopping the compacted material, and sintering somewhat below the melting temperature. The impurities in the bauxite act as sintering agents, leading to very fine crystal size and extremely high toughness (Table 2.3). The final abrasive product generally has rounded edges without sharp corners [13]. This abrasive is applied to heavy-duty grinding operations.

The introduction of mixed alumina–zirconia abrasives has had a profound effect on heavy-duty grinding operations. Alumina and zirconia show very limited mutual solubility and form a simple eutectic at approximately 42wt% zirconia (ZrO_2). Although ZrO_2 has intrinsically a hardness value about half that of Al_2O_3, this eutectic structure is very tough because of the ability of the softer dispersed zirconia phase to stop cracks, preventing the grains from fracturing under quite high loads and so both allowing them to be used under more arduous conditions and to last longer at a given load. Another factor contributing to the superior performance of alumina zirconia abrasives for heavy-duty grinding, relative to fused or sintered aluminas, is the higher melting point of ZrO_2 (2720°C) as compared with that of Al_2O_3 (2040°C), which suggests a greater degree of chemical stability [14]. Mixed alumina-rich abrasives, consisting of distinct hard Al_2O_3 and tough Al_2O_3–ZrO_2 eutectic are produced with zirconia contents up to the eutectic composition by fusing calcined bauxite, zircon sand, coke and iron in an electric arc furnace. The melt is rapidly quenched and solidified to a fine dendritic structure by pouring it in a thin layer over a water-cooled steel plate and crushing. Different ZrO_2 contents give abrasives with different mechanical properties, materials richer in Al_2O_3 tending to be harder and more friable and those nearer the eutectic being tougher and less friable. The Al_2O_3–ZrO_2 eutectic is a very interesting material since, on quenching, the zirconia crystals may be locked into their high-pressure form and revert to the low-pressure form with an increase in volume if a crack approaches, thus enhancing toughness by filling the crack and making it more difficult for it to move and split the material [15,16].

So called 'sol-gel' abrasives represent one of the most recent developments in the technology of abrasive synthesis [17]. Such materials are made neither by fusing nor by sintering, but instead by converting a colloidal dispersion of hydrosol ('sol') containing goethite ($Al_2O_3{\cdot}H_2O$) to a semi-solid 'gel', drying this gel to a glassy state, crushing to the required grain size, and firing at 1300°C. The final product consists of aluminum oxide grains with a randomly oriented microcrystalline structure. These abrasives were originally applied to heavy-duty operations with coated abrasives, but aluminum oxide abrasives produced by a similar processing technology have also been shown to provide dramatic performance improvements, compared to fused aluminum oxide abrasives, for grinding of steels with vitrified wheels.

Silicon carbide is made by reducing sand (SiO_2) with excess coke (C) in an electric furnace at temperatures above 2000°C, according to

$$SiO_2 + 3C \rightarrow SiC + 2CO$$

The desired product is the hexagonal form of silicon carbide (α-SiC), which is green-to-black in color, although the final reaction mass contains a mixture of unreacted coke, partly reduced 'firesand', and silicon carbide. This is carefully separated and the silicon carbide fraction collected for further processing, the firesand and coke being returned to the furnace for further treatment as part of a subsequent charge. Green silicon carbide is purer than black and, being a semiconductor, is a premium product also used to make heating elements for furnaces. The black material is preferred for grinding on a cost basis, although it is slightly less hard.

Both varieties of silicon carbide are intrinsically harder than alumina and comparable in friability to the hardest alumina abrasives (Table 2.3 and Fig. 2.4), and this combination of physical properties would suggest that silicon carbide might be better than alumina oxide for fine grinding processes. This is generally so for non-ferrous metals and for most ceramics, but silicon carbide is inferior for most ferrous applications, because of its chemical reactivity with iron and steel alloys, leading to poor attrition resistance and low grinding ratios (Chapter 8). Silicon carbide is, however, better for some hard cast irons, where the high carbon content in the metal minimizes chemical interaction with the wheel.

2.5 SUPERABRASIVE MATERIALS

Superabrasive materials include diamond and cubic boron nitride. Diamond is the hardest known material, and cubic boron nitride is the second hardest. As an abrasive, diamond is used in both its natural and its synthetic forms, although the trend is generally towards the synthetic material. Boron nitride, in both its cubic and its soft hexagonal forms, is a synthetic material.

In the case of natural diamonds. their shape and size are determined by nature

during their geological formation, although they can be reshaped by man using mechanical and thermal methods. For synthetic diamond, the same reshaping techniques can be used, but their intrinsic strength and structure can be altered by varying the processing conditions. Synthetic diamond is produced by subjecting graphite to high temperatures at extremely high pressures in the presence of a catalyst solvent such as nickel or other metals from group VII of the periodic table [18–21]. With nickel as a catalyst, operating conditions might be about 2000°C at 75–95 kbar. Depending on the particular temperature, pressure, and processing time, diamonds are made with varying crystal sizes and structures. Synthetic diamond abrasives range from weak, friable, irregularly shaped polycrystalline grains with a skeletal structure to tough blocky-shaped cubo-octahedral single crystals. The weaker shapes are applied mainly to grinding of cemented carbides with resin-bonded wheels. For this application, the diamonds are usually coated with nickel comprising about 55% by weight of the grain and coating. The purpose of the coating is to more strongly hold the diamond grit in the resin binder, in addition to providing some protection from the atmosphere. Stronger blockier monocrystalline diamond grits are used mainly with metal bonds for cutting of ceramics, stone, glass, and other hard brittle materials.

In spite of its extreme hardness, diamond had been found not to be economical for grinding of most ferrous materials, except for some hard cast irons, owing to graphitization and carbon diffusion into the iron causing excessive diamond wear. Cubic boron nitride has emerged as an important alternative superabrasive for grinding of steels and some non-ferrous high-strength alloys. Boron nitride was first made as the hexagonal polymorph, isostructural with and soft and slippery as graphite. This structural analogy with graphite, combined with the fact that boron is chemically very similar to carbon, inspired the thought that it might be possible to synthesize a cubic form of boron nitride analogous to diamond, and this was achieved at temperatures of 1500–2000°C at pressures in the range 50–90 kbar (5–9 GPa) using alkali metals as catalytic solvents [22].

Almost all CBN grits produced today are monocrystalline, although polycrystalline (microcrystalline) abrasives with submicron crystal size have also been recently introduced. In its polycrystalline form, CBN is claimed to be significantly tougher. Monocrystalline CBN grits tend to be blocky shaped with sharp edges and smooth faces, which make bonding difficult. As with diamond, a nickel coating is added to retain the grits more strongly in resin-bonded wheels.

In comparison with diamond one important advantage of CBN is its thermal stability. Both diamond and CBN are stable in vacuum up to temperatures in excess of 1400°C. In normal atmosphere, a B_2O_3 protective layer on CBN prevents oxidation up to 1300°C, and no conversion from the cubic to hexagonal form occurs up to 1400°C. By contrast, diamond is thermally stable only to a much lower temperature of about 800°C in normal atmosphere. An important consequence of this is related to the possibilities for vitrified superabrasive wheels. CBN wheels with vitrified bonds can be fired to a much higher temperature than diamond, and so a much wider range of vitreous bonds can be considered for their manufacture. Some CBN grits are specially coated to protect their surface from chemical reaction above 800°C with the alkali and water present in most glass frits used in vitrified wheel manufacture. While vitrified bonds are only occasionally used with diamond, they are becoming an increasingly significant factor with CBN.

2.6 BOND MATERIALS

Abrasive grains are held together with various kinds of bond materials. In general, the bond must be strong enough to withstand grinding forces, temperatures, and centrifugal forces without disintegrating, while resisting chemical attack by the cutting fluid. Additional bond requirements may include wheel rigidity, and the ability to retain abrasive grains during cutting yet release dulled grains.

According to the wheel marking system in Fig. 2.1, there are six general types of bond materials for conventional abrasive wheels: resinoid (including reinforced), shellac, oxychloride, rubber (including reinforced), silicate, and vitrified. Most conventional abrasive wheels have either vitrified or resinoid bonds. Superabrasive wheels (Fig. 2.3) are produced with three bond types: resinoid, vitrified, and metal.

Vitrified wheels probably account for about half of all conventional abrasive wheels, although the trend towards higher wheel speeds has led to some replacement by resinoid wheels, especially for heavy-duty grinding. Historically, the use of vitrified wheels was restricted to peripheral speeds of about 30 m/s (6000 ft/min) owing to strength limitations, although methods for wheel reinforcement now make it possible to use these wheels at peripheral speeds up to 80–90 m/s (16,000–18,000 ft/min). The highest speed used in production with vitrified wheels is at present 120 m/s (24,000 ft/min).

Vitreous bonds are formed from mixtures of a clay, a feldspar, and a frit, normally using locally available materials, in amounts mainly determined by the nature of the wheel to be built but also affected by the mineralogy and detailed chemistry of the clays and feldspars used, in particular minor phases and trace elements present. The frit is man-made and its composition is under better control. Such mixtures soften and melt in the temperature range 950 to 1400°C with mixtures richer in clay melting at higher temperatures, those with more frit melting at lower temperatures. It is, thus, possible to prepare bond mixtures with different viscosities, and hence different surface tensions at a given temperature, and so tailor the bond to the required structure of the final wheel. In particular, it becomes possible to help control the porosity in, and provide the strength to, the wheel by careful choice of bonding mix. The mixtures are prepared by milling the raw materials together with about 1–5% water containing an organic binder, such as dextrin, until a plastic mass ensues.

Vitreous bonds are almost always used with alumina grits, and this plastic mixture is next added to between two and six times its weight of the requisite abrasive. Again, the exact weight percentage depends on the nature of the wheel and the use to which it will be put and the clays and feldspars used. A combustible filler, such as sawdust, may be added if a very porous wheel is required. The mix is pressed to the required shape, dried, and fired in a traveling kiln to a temperature in excess of 1260°C in a regime extending over some days. The heating stage is relatively rapid, taking 1 to 2 days to reach the maximum temperature, which is held for about 12 hours, but

cooling must be slow and carefully controlled to avoid building thermal stresses into, or even cracking, the wheels. Very large wheels can take weeks to cool.

At the firing temperature, the bonding mix melts, partly wets the abrasive grits, and surface tension pulls them together [23]. At the same time, chemical reactions occur at the grit–melt interface with interpenetration of grit and melt, the β-Al_2O_3 phase in the white grits is dispersed into the surrounding matrix (removing a potential source of weakness in the grit particles), and a titania-rich phase is exsolved from the brown Al_2O_3 grains, causing them to turn blue. On subsequent cooling, glassy 'necks' of solidified bonding material, called bond posts, develop between the grains holding them firmly together, and these are anchored both by a mechanical bond, where the molten material has flowed into irregularities in the grit surfaces, and by chemical bonds due to the new phases formed at the grit–bond interface [24]. An example of a vitrified wheel structure is shown in Fig. 2.5.

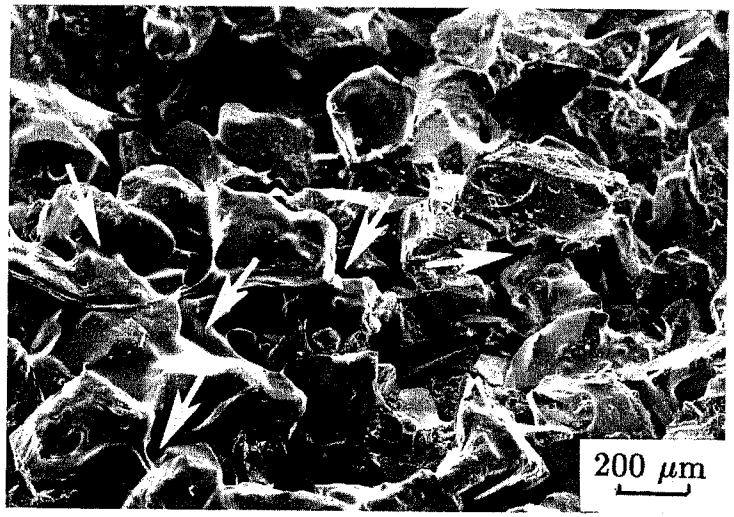

Fig. 2.5 — SEM micrograph of vitrified wheel 32A54I8VX. Abrasive is monocrystalline alumina. Arrows point to bond posts.

Resinoid-bonded wheels are produced by mixing abrasive grains with phenolic thermosetting resins and plasticizers, molding to shape, and baking (curing) at 150–200°C. The bond hardness is varied by controlling the amount of plasticizer and by addition of fillers. Conventional abrasive resinoid wheels are widely used for heavy-duty grinding (snagging) operations because of their high strength and ability to withstand shock loads. Another important application is for cut-off wheels, which are usually reinforced with fiberglass for added strength and high-speed operation up to about 100 m/s (20,000 ft/min). For superabrasive wheels, resinoid bonds are the most popular, the most important applications being with diamond abrasives for grinding of cemented carbides and CBN for grinding of steels.

Resinoid wheels are susceptible to chemical attack by alkaline cutting fluids which adversely affect their strength, especially with prolonged exposure at elevated temperature [25]. The fluid not only lowers the strength of the resin itself, but can weaken its bonding to the abrasive, which is one reason why aluminum oxide grains for resinoid wheels are specially treated with a thin coating. Grinding fluid attack may not be a problem with heavy-duty and cut-off wheels, insofar as they are often used dry. The strength of superabrasive resinoid wheels generally does not depend on the resinoid bond, since it is only in a thin outer layer. However, alkaline grinding fluids will likely degrade the wheel performance over a period of time.

Rubber bonds consist of vulcanized natural or synthetic rubber. The main applications are thin wheels for wet cut-off operations to produce nearly burn-free cuts, and regulating wheels for centerless grinders. Rubber wheels were once popular for finishing operations on bearings and cutting tools, but their use for these purposes has declined. The manufacture of thin rubber-bond wheels involves mixing together the rubber and abrasive with sulfur added as a vulcanizing agent, rolling out in sheets to the required thickness, cutting out the required shape, and vulcanizing under pressure at 150–275°C. Thick wheels can be manufactured in a similar way, but by stacking of thin sheets after cutting.

Silicate-bonded wheels are manufactured by mixing sodium silicate with abrasive, tamping in a mold, drying and baking. The historical advantage of silicate in comparison with vitrified wheels is the much lower processing temperature and shorter heating cycles. At one time, the silicate process was popular with small grinding wheel manufacturers lacking facilities for producing vitrified products. The process might still be occasionally used for producing extra-large slow-speed wheels for some sharpening and finishing operations.

Shellac is a natural organic material which is only rarely used today as a bond material. The wheels can be manufactured by mixing abrasive grain with shellac, shaping under pressure in heated molds, and baking. At one time this bond was used for flexible cut-off wheels, which is probably why they were referred to as elastic wheels. The use of shellac-bond wheels is mainly for fine finishing of mill rolls, camshafts, and cutlery.

Another less common type of bond is oxychloride, which is a cold-setting cement from a mixture of magnesium oxide and an aqueous solution of magnesium chloride. Apparently it was very popular about a hundred years ago, but its only use today might be for disk grinding. It is susceptible to chemical attack by grinding fluids, so it is used dry.

Metal bonds are extensively used with superabrasive wheels. The most common are from sintered bronze, which are produced by powder metallurgy methods. Variation of the wheel grade is controlled by adding modifiers and altering the bronze composition. Other powder metal bonds, which are generally stronger, include iron and nickel. Segmented diamond saws for cutting stone and granite typically have sintered nickel bonds. Tungsten powder infiltrated with a low melting point alloy is used in diamond wheels for grinding diamond tools. Still stronger bonds consisting of WC–Co cemented carbide are used in diamond abrasive tools for geological drilling.

A different type of metal bond for superabrasive wheels is manufactured by electroplating. These grinding wheels consist of a single layer of diamond or CBN held in place on a preform by an electroplated nickel coating. Electroplated superabrasive wheels are generally less expensive than bonded types, insofar as they contain less diamond or CBN. An important advantage is the ability to produce profiled wheels with sharp corners and radii. Extremely thin metal-bonded diamond wheels for slicing and dicing of electronic materials are produced by electroplating a single layer of diamond onto a substrate which is subsequently discarded.

2.7 WHEEL COMPOSITION AND PHASE DIAGRAM

In sections 2.2 and 2.3, the wheel composition was described in terms of its marking system. The grinding wheel can, however, be described more objectively and with more references to its structure and composition in terms of a 'grinding wheel phase diagram'. If we neglect possible additions of fillers and grinding aids, a grinding wheel can be considered as a three-phase system consisting of abrasive grains, bonding medium, and porosity. We can then write

$$V_g+V_b+V_p = 100 \qquad (2.6)$$

where V_g, V_b and V_p are the volume percentages of the grit, bond and pore or soft phases, respectively. This composition relationship can conveniently be represented in the form of a standard, equilateral-triangle-shaped three-phase diagram, as shown in Fig. 2.6 [26]. In such a diagram, each apex represents 100% of one component

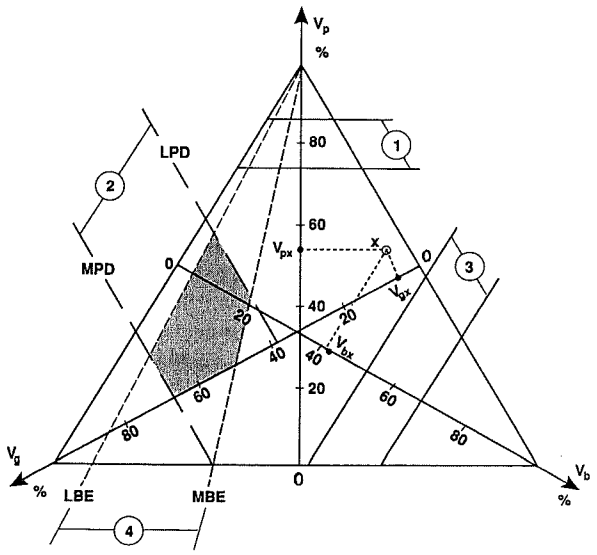

Fig. 2.6 — Grinding wheel phase diagram [26].

with the opposite side corresponding to 0% and intermediate percentages represented by the fractional distance from the side to the apex. Three axes can be drawn from the apexes to the opposite sides to illustrate this relationship, and these are shown in Fig. 2.6.

Lines in the phase diagram drawn perpendicular to these axes, and so parallel to the sides, represent compositions all with the same percentage of the component represented by the opposite apex. Thus, lines ① represent compositions all with V_p=75% (lower line) or 86% (upper line), lines ② with V_g=68% (MPD) or 38% (LPD), and lines ③ with V_b=54% or 68%. Such lines are known as 'iso-lines', either iso-porosity ① or iso-grain ② or iso-bond ③. Note that the sum of the percentages of the other two components is constant across an iso-line but the individual percentages vary. Any point 'x' within the triangle in Fig. 2.6 represents a specific wheel composition, i.e. V_{gx}, V_{bx}, and V_{px}.

Also of some significance are the lines shown as ④ in Fig. 2.6. These are lines that connect an apex to points on the opposite side and represent sets of compositions with a constant ratio of the components at the ends of the side and varying amounts of the apex component. Thus, lines ④ represent compositions with constant grit-to-bond ratios, of about 12:1 (LBE) and 3:1 (MBE), but with different porosity contents.

In practical terms, iso-grain lines, corresponding to particular grain volume percentages and varying amounts of bond and pore phases, generally define the 'structure' or 'packing number' in the wheel markings for conventional wheels (Fig. 2.1) or the concentration number for superabrasive wheels (Fig. 2.3). Iso-porosity lines are sometimes considered to indicate the 'wheel hardness' or 'grade' of conventional wheels, but this will be discussed further below. Note that a filler may take the place of the pore phase in a resinoid-bonded wheel.

Actual wheel compositions do not cover the whole composition range represented by the phase diagram but are restricted to a limited range by technological and practical factors. For example, a typical useful composition range for conventional vitreous-bonded wheels is represented by the shaded region in Fig. 2.6, and shown expanded in Fig. 2.7. This is bounded by two iso-grain lines (MPD and LPD) and three constant ratio lines (LBE, MBE, and the V_g axis where $V_p=V_b$). The limiting upper iso-grain line, the 'maximum packing density' or MPD line, represents the natural maximum packing density imposed by the shapes and sizes of the abrasive grains, and its exact value (position on the diagram) will depend on the shape and size distribution of the abrasive grains used. The 'lower packing density' or LPD line is linked to the condition at which there are just enough grit–grit contacts, with their attendant bond posts, to give the required strength to the wheel. Again, the exact position of this line depends on details of the abrasive grains used. The 'maximum bond equivalent' or MBE line corresponds to the bond–grit ratio above which the bond simply coats the grit particles without forming additional bond posts, while the 'lower-bond equivalent' or LBE line is again associated with the provision of a minimal amount of bond phase to give the required strength. The shaded area in Fig. 2.6 is bounded by V_g=68% for the MPD line, V_g=38% for LPD, V_b/V_g=0.31 for MBE and V_b/V_g=0.08 for LBE, but the actual boundaries for other types of wheel will depend on the particular abrasive–bond system used.

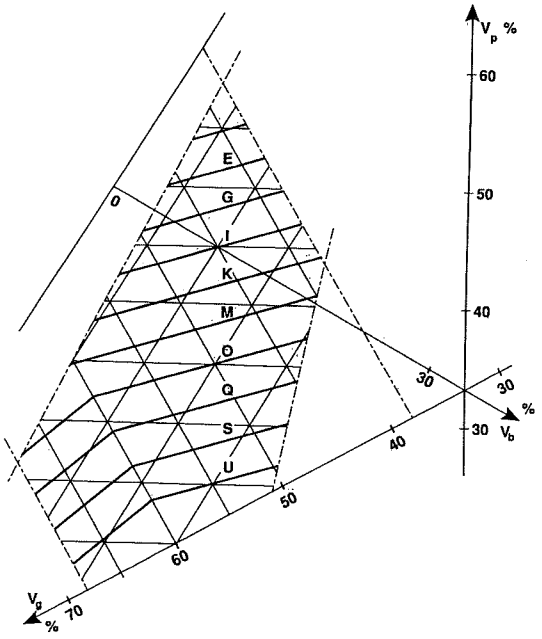

Fig. 2.7 — Shaded region of phase diagram from Fig. 2.6 showing iso-grade loci [26].

Most wheel manufacturers use different bond mixes and proportions of abrasive and bond to achieve a given letter grade (hardness) of wheel, and so iso-grade lines do not usually coincide with iso-porosity lines. One manufacturer's gradings for wheels of different compositions are plotted in Fig. 2.7. Wheels with the same grade plot as straight lines against overall composition which are uniformly inclined to the iso-porosity lines, rather than coinciding with them, and they show a marked discontinuity in relative slope at V_g=60%. Below this grit content, i.e. in the majority of useful wheels, the percentage porosity can be expressed as a function of grade number in the form

$$V_p(\%) = \frac{2(99.5 - 2n) - V_g}{3} \tag{2.7}$$

where n is an integer ($n = 1, 2, 3, 4, \ldots$) corresponding to the letter grade (E, F, G, H, ...), respectively. If the structure number relationship of Eq. (2.5) applies, the wheel porosity can be expressed in terms of the structure number and letter grade by the relationship

$$V_p(\%) = 45 + \frac{S - 2n}{1.5} \tag{2.8}$$

Accordingly, wheels with the same grade number but containing less grain (higher S value) should be more porous, and this is in accordance with the predictions of the phase diagram.

Again, each manufacturer uses his own characterization standards to arrive at his particular wheel grade and structure number. Moreover, bond formulations and processing methods, as indicated earlier, vary from one manufacturer to another, and so wheels from different manufacturers, although with apparently identical abrasive grit, bond and pore contents and having the same indicated letter grade and structure number, can be expected to perform differently. The grinding wheel marking system has been standardized, as also are the abrasive grits to some extent, but the wheels produced are not.

2.8 GRINDING WHEEL TESTING

Various testing procedures have been developed for evaluating grinding wheel performance, checking quality in wheel production, and ensuring wheel safety. Wheel performance is generally evaluated by actual grinding tests, as will be seen in Chapter 8. Here we will be concerned with non-grinding tests for identifying inherent wheel properties.

One of the more elusive characteristics of a grinding wheel is its hardness or grade. As seen in the previous section, a harder-grade wheel having a given abrasive content contains more binder and less porosity. Therefore, harder wheels should be stronger, and the abrasive grits should be more firmly held by the binder.

Hardness testing of vitrified grinding wheels was originally introduced not for the purpose of checking the wheel grade, but rather for actually grading the wheel. Owing to lack of technical sophistication for controlling the vitrified wheel manufacturing process, wheels were assigned grades only after their manufacture. The test method consisted of scratching the grinding wheel with a screwdriver-like hand tool. The operator would determine the wheel grade by the resistance he felt and the sound emitted.

Similar modern methods for testing and grading of grinding wheels involve measurement of forces while removing wheel material with a tool. One such test involves the use of a triangular-pointed tool to scratch a groove in a wheel with the depth of penetration set equal to the grit dimension [27]. Force pulses are measured which are each assumed to be associated with dislodgement of a single grit, and the average force is taken as an indication of wheel grade. However, grit fracture is also likely to occur in addition to dislodgement, especially with harder wheels. Another test uses a conical metal tool instead of a grooving tool [28]. The conical tool is free to rotate, so it crushes the wheel instead of being ground away as it is fed across the rotating wheel face. These two test methods, groove scratching and crushing, were found to agree quite well in their ability to distinguish between wheels of different hardness [29]. However, the measured forces with both methods are dependent not only on the bond strength but also on grit toughness, so the measured grade indication cannot be generally adopted as an intrinsic wheel grade property.

Numerous other wheel grade tests have been proposed, but only a few have been used to a significant extent. Two relatively simple ones, which were adopted many years ago in industry, measure penetration depths due to a rotating chisel driven vertically into the wheel or by sandblasting under standard conditions. While these

tests provide a relative indication of bond strength and its variation over the wheel surface, the results are difficult to physically interpret.

A more fundamental parameter which has been proposed for characterizing wheel grade is the elastic modulus [26]. Relatively simple methods have been developed for determining the elastic modulus based upon measuring the natural frequency of a grinding wheel excited by impact [26,30]. For a disk (wheel) of outer diameter d_s with a central hole of bore diameter d_0, the relationship between the elastic modulus E and the frequency f for the two nodal diameter vibration mode is given to a good approximation for $d_0/d_s<0.25$ by [26]:

$$E = \frac{1.07(1-\nu^2)\rho d_s^4 f^2}{b^2\left[1-\left(\frac{d_0}{d_s}\right)^2\right]} \tag{2.9}$$

where ρ is the mass density, ν is Poisson's ratio, and b is the disk thickness.

Experimental results are presented in Fig. 2.8 for both the elastic modulus and

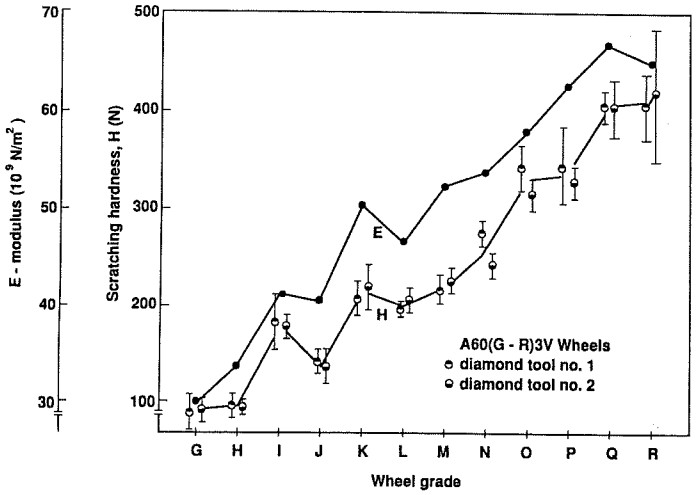

Fig. 2.8 — Elastic modulus and groove-scratching hardness for a series of vitrified wheels of differing grades [26].

the groove-scratching hardness for a series of vitrified wheels of differing grades [26]. Both tests show the same relative trend of increasing 'hardness' with letter grade. Good correlation was also found with the popular sandblast hardness test. Advantages of the sonic test are that it does not consume any wheel, is much simpler to perform, and the measured modulus is insensitive to grit toughness. The discontinuities observed in the results in Fig. 2.8 indicate deviations in wheel hardness.

On the basis of these results, it would appear that a rational wheel grade scale might be based upon elastic modulus. From tests on aluminum oxide wheels over a range of compositions, it has been found that iso-modulus lines on a ternary phase diagram are as shown in Fig. 2.9, which are somewhat different than the iso-grade

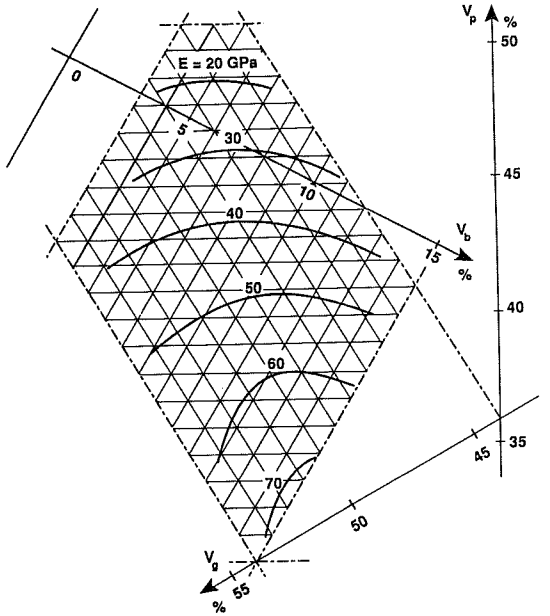

Fig. 2.9 — Iso-modulus loci for vitrified wheels shown on the ternary phase diagram [26].

lines in Fig. 2.7. Although this proposed grading system has not been adopted, the sonic testing of grinding wheels has become popular mainly as a tool for quality control. Wheel manufacturers use this method for monitoring their production process, and some wheel users have adopted it for acceptance testing and matching of wheels. The test method is supposedly applicable to both vitrified- and resinoid-bond wheels [26], although it is reported not to function well on resinoid wheels because of their lower elastic modulii and higher damping [30]. Vitrified wheels tend to display more variability in grade and grinding performance, and the use of this test method has assisted wheel manufacturers in their efforts to provide more consistent products.

Aside from the wheel grade, another important wheel property is strength. Grinding wheels are operated at speeds which generate high stresses due to centrifugal loading. In order to ensure the safety of the operator and the machine, it is essential that wheel speeds be maintained within safe limits. For this reason, maximum operating speeds are clearly indicated on all grinding wheels, and the

wheels are proof tested at faster speeds (minimum 1.2–1.5 times their rated speed depending on bond type) to ensure safety [31]. Operating speeds on grinding machines have been historically limited by wheel strength, rather than by the process itself. The search for more efficient grinding methods by employing higher wheel speeds prompted the development of stronger wheels with higher bursting speeds. Some approaches which have been explored for raising allowable wheel speeds include wheel reinforcemnt, segmental wheel designs, solid center wheels, higher-strength bonds, and higher core strengths.

Speed and safety considerations are an especially important factor with vitrified wheels. Since these wheels are brittle bodies, they can be expected to burst when the rotationally induced tensile stress reaches a critical value, releasing loose fragments with only a negligible portion of their kinetic energy absorbed by fracture. Considering a grinding wheel in the form of a disk of diameter d_s with bore diameter d_0 rotating at a peripheral velocity v_s, the maximum tensile stress developed, which is a tangential (hoop) stress at the bore diameter, can be written as [32]

$$\sigma_{max} = \rho\left(\frac{3+\nu}{4}\right)\left[1+\left(\frac{1-\nu}{3+\nu}\right)\left(\frac{d_0}{d_s}\right)^2\right]v_s^2 \qquad (2.10)$$

where ρ is the mass density and ν is Poisson's ratio. For typical ratios of bore to outer diameter, the second term within the brackets is generally much less than unity, which means that the maximum tensile stress developed is relatively insensitive to the bore and hole diameters and proportional to the velocity squared.

Aside from centrifugal forces, additional stresses are induced by wheel clamping and grinding forces [33,34]. In general, these effects appear to be much less significant than the rotational stresses, although bursting speeds of improperly clamped wheels can be significantly lowered [35]. With thin resinoid (reinforced) wheels, sideways loading tending to bend the wheel may be a more significant factor than centrifugal loading. The bending strength depends on the orientation of the fibre-reinforcing layers [36]. The grinding fluid may also lower resinoid wheel strength [25].

Some results for bursting speeds of non-reinforced vitrified grinding wheels, compiled by one manufacturer over a number of years, are summarized in Fig. 2.10. According to Eq. (2.10), the observed bursting speeds of 90 m/s (18,000 ft/min) to 130 m/s (23,000 ft/min) would correspond to maximum tensile stresses of about 13 MPa (1900 lb/in^2) to 26 MPa (3800 lb/in^2), which are comparable to measured short-time tensile strengths [37]. These bursting speeds far exceed the normal operating limit of 30 m/s (6000 ft/min) with these wheels, and the relative margin of safety is even bigger when compared in terms of strength. It should be noted, however, that these results are for average bursting speeds. As is typical of many brittle materials, the tensile strength of vitrified wheels is found to exhibit significant scatter which can be described by a Weibull distribution [37]. Furthermore, the grinding fluid and moisture in the air may also degrade wheel strength over a period of time. The higher strengths observed with harder-grade wheels (Fig. 2.10) are a consequence of the higher bond content which provides bigger bond bridges with larger cross-sections. Finer-grit wheels may be stronger owing to proportionally smaller defect sizes for initiation of brittle fracture.

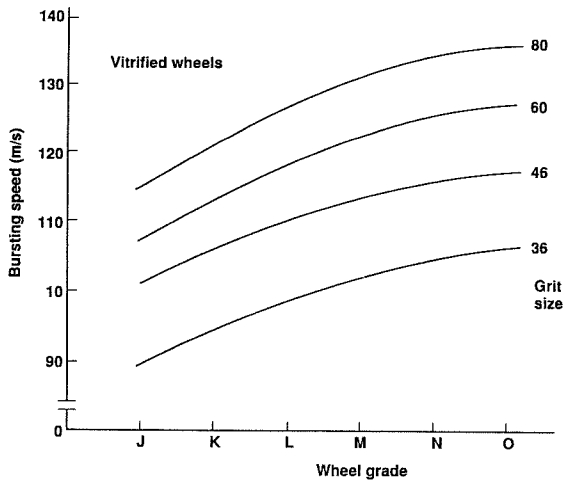

Fig. 2.10 — Peripheral bursting speeds for vitrified grinding wheels.

A more fundamental approach to ensuring reliability of grinding wheels against failure combines fracture mechanics, finite element stress analysis, and Weibull statistics [38]. With this method, bonded abrasive specimens are tested in four-point bending to measure the fracture strength, its statistical variability, and its time-dependent degradation (static fatigue). The stress distribution in the grinding wheel during operation is obtained using a finite element analysis. The overall time-dependent probability of wheel failure can be statistically predicted by coupling the stress distribution over the wheel with the fracture-strength results, while taking into account the increased probability of encountering strength-impairing flaws in larger stressed volumes. The results of this analysis provide a rational basis for overspeed proof testing to ensure that a grinding wheel will not fail during its useful life.

Bursting of a wheel operating within its rated speed limit is an extremely unlikely event. The causes of wheel failure are generally associated with overspeeding, shock loading, improper mounting, and mishandling [35]. With proper guarding, a wheel failure should not pose a serious danger to the operator.

REFERENCES

[1] 'Markings for Identifying Grinding Wheels and Other Bonded Abrasives', American National Standard ANSI B74.13—1982.

[2] 'Specifications for the Size of Abrasive Grain-grinding Wheels, Polishing and General Industrial Uses', American National Standard ANSI B74.12—1976 (R1982).

[3] 'Specifications for Grading of Abrasive Microgrits', American National Standard ENSI B74.10 (R1983).

4] Malkin, S. and Anderson, R. B., 'Active Grains and Dressing Particles in Grinding', *Proceedings of the International Grinding Conference*, Pittsburgh, 1972, p. 161.
5] Coes, L., Jr., *Abrasives*, Springer-Verlag, New York, 1971, Chapter 3.
6] 'Checking the Size of Diamond Abrasive Grain', American National Standard ANSI B74.16—1982.
7] 'Specifications for Grading of Diamond Powder in Sub-sieve Sizes', American National Standard ANSI B74.20—1981.
8] Ueltz, H. G. G., 'Abrasive Grains — Past, Present, and Future', *Proceedings of the International Grinding Conference*, Pittsburgh, 1972, p. 1.
9] 'Ball Mill Test for Friability of Abrasive Grain', American National Standard B7418—1965.
0] Cadwell, D. E. and Duwell, E. J., 'Evaluating Resistance of Abrasive Grits to Comminution', *Amer. Ceram. Soc. Bull.*, **39**, 1960, p. 663.
1] Brecker, J. N., Komanduri, R. and Shaw, M. C., 'Evaluation of Unbonded Abrasive Grains', *Annals of the CIRP*, **22**/2, 1973, p. 219.
2] Brecker, J. N., 'The Fracture Strength of Abrasive Grains', *J. Eng. Ind., Trans. ASME*, **96**, 1974, p. 1253.
3] Komanduri, R. and Shaw, M. C., 'Scanning Electron Microscope Study of Surface Characteristics of Abrasive Materials', *J. of Eng. Mats. Tech., Trans. ASME*, **96**, 1974, p. 145.
4] Coes, L., Jr., *Abrasives* Springer-Verlag, New York, 1971, Chapter 8.
5] Lange, F. F., Transformation Toughing — 4. Fabrication, Fracture Toughness, and Strength of Al_2O_3–ZrO_2 Composites', *J. Mater. Sci.*, **17**, 1982, p. 247.
6] Hever, A. H., 'Transformation Toughening in ZrO_2-containing Ceramics', *J. Am. Ceram. Soc.*, **70**, 1987, p. 689.
7] Leitheiser, M. A. and Sowman, H. G., 'Non-fused Aluminum Oxide-based Abrasive Mineral', U.S. Patent 4,314,827, 9 February 1982.
8] Bundy, F. P., Hall, H. T., Strong, H. M. and Wentorf, R. F., Jr., 'Man-made Diamonds', *Nature*, **176**, 1955, p. 55.
9] Coes, L., Jr., *Abrasives* Springer-Verlag, New York, 1971, Chapter 10.
0] Komanduri, R. and Shaw, M. C., 'Surface Morphology of Synthetic Diamonds and Cubic Boron Nitride', *Int. J. Mach. Tool Des. Res.*, **14**, 1974, p. 63.
1] O'Donovan, K. H., 'Synthetic Diamond', *Annals of the CIRP*, **24**/1, 1975, p. 265.
2] Wentorf, R. H., 'Synthesis of Cubic Form of Boron Nitride', *J. Chem. Phys.*, **34**, 1961, p. 809.
3] Brecker, J. N., 'Analysis of Bond Formation in Vitrified Abrasive Wheels', *J. Amer. Ceram. Soc.*, **57**, 1974, p. 486.
4] Kingery, W. D., Sidhwa, A. P. and Waugh, A., 'Structure and Properties of Vitrified Bonded Abrasives', *Amer. Ceram. Soc. Bull.*, **42**, 1963, p. 297.
5] Ellendman, M., 'How Coolants Affect the Performance of Resin-bonded Abrasive Wheels', *Machine and Production Engineering*, **115**, No. 2975, 1969, p. 812.
Peters, J., Snoeys, R. and Decneut, A., 'Sonic Testing of Grinding Wheels', *Proceedings of the Ninth International Machine Tool Design and Research Conference*, 1968, p. 1113.

[27] Peklenik, J. and Opitz, H., 'Testing of Grinding Wheels', *Proceedings of the Third International Machine Tool Design and Research Conference*, 1962, p. 163.
[28] Colwell, L. V., Lane, R. O. and Soderlund, K. N., 'On Determining the Hardness of Grinding Wheels', *J. of Eng. for Ind., Trans. ASME*, **84**, 1962, p. 113.
[29] Peklenik, J., Lane, R. and Shaw, M. C., 'Comparison of Static and Dynamic Hardness of Grinding Wheels', *J. of Eng. for Ind., Trans. ASME*, **86**, 1964, p. 294.
[30] Brecker, J. N., 'Grading Grinding Wheels by Elastic Modulus', *Proceedings, First North American Metalworking Research Conference*, Vol. 3, 1973, p. 149.
[31] 'Safety Requirements for the Use, Care and Protection of Abrasive Wheels', American National Standard ANSI B 7.1—1978.
[32] Timoshenko, S. and Goodier, J. N., *Theory of Elasticity*, 2nd edn, McGraw-Hill, New York, 1951, p. 71.
[33] Miyamoto, H., Shibahara, M., Oda, J. and Kazama, E., 'Three-dimensional Stress Analysis of Grinding Wheel', *Bull. Japan Soc. of Prec. Engg*, **4**, 1970, p. 79.
[34] Oda, J., Shibahara, M. and Miyamoto, H., 'Calculation of Stresses in Grinding Wheel Caused by Grinding Force', *Bull. Japan Soc. of Prec. Engg*, **6**, 1972, p. 25.
[35] Sabberwal, A. J. P., 'Review of Codes of Practice on Safety in Grinding', *Annals of the CIRP*, **21**/2, 1972, p. 187.
[36] Rajagopal, S. and Kalpakjian, S., 'Properties of Reinforced Abrasive Disks in Flexure', *J. Eng. Ind., Trans. ASME*, **99**, 1977, p. 318.
[37] Yamamoto, A., 'Strength and Static Fatigue of Vitrified Grinding Wheels under Various Environments. II', *Bull. Japan Soc. of Prec. Engg*, **10**, 1976, p. 45.
[38] Ritter, J. E., Jr., 'Assuring Mechanical Reliability of Ceramic Components', *J. Ceramic Society Japan*, **93**, 1985, p. 341.

BIBLIOGRAPHY

Armarego, E. J. A. and Brown, R. H., *The Machining of Metals*, Prentice-Hall, Englewood Cliffs, NJ, 1969, Chapter 11.
Coes, L., Jr., *Abrasives*, Springer-Verlag, New York, 1971.
DeVries, R. C., 'Cubic Boron Nitride: Handbook of Properties', GE Report No. 72CRD178, 1972.
Drozda, T. J. and Wick, C., Eds, *Tool and Manufacturing Engineers Handbook, Vol.* 1, *Machining*, 4th edition, SME, Dearborn, 1983, Chapter 11.
Jacobs, F. B., *Abrasives and Abrasive Wheels*, Henly, New York, 1919.
Komanduri, R. and Shaw, M. C., 'Scanning Electron Microscope Study of Surface Characteristics of Abrasive Materials', *J. of Eng. Matls. Tech., Trans. ASME*, **96**, 1974, p. 145.
Komanduri, R. and Shaw, M. C., 'Surface Morphology of Synthetic Diamonds and Cubic Boron Nitride', *Int. J. Mach. Tool Des. Res.*, **14**, 1974, p. 63.

Lewis, K. B. and Schleicher, W. F., *The Grinding Wheel*, 3rd edn, The Grinding Wheel Institute, Cleveland, 1976.
Metzger, J. L., *Superabrasive Grinding*, Butterworths, London, 1986, Chapters 3 and 4.
O'Donovan, K. H., 'Synthetic Diamond', *Annals of the CIRP*, **24**/1, 1975, p. 265.
Peters, J., Snoeys, R. and Decneut, A., 'Sonic Testing of Grinding Wheels', *Proceedings of the Ninth International Machine Tool Design and Research Conference*, 1968, p. 1113.
Pugh, H. C. and Stark, C., 'Methods for Testing Grinding Wheel Quality', *Proceedings, Twelfth North American Manufacturing Research Conference*, 1984, p. 339.
Stewart, I. J., 'On the Safety of High Speed Grinding', *Proceedings of the International Grinding Conference*, Pittsburgh, 1973, p. 649.
Veltz, H. F. G., 'Abrasive Grains — Past, Present, and Future', *Proceedings of the International Grinding Conference*, Pittsburgh, 1973, p. 1.
Whitney, E. D. and Shepler, R. E., 'Ceramics in Abrasive Processes', *Materials Science Research*, **7**, 1974, p. 167.

3

Grinding geometry and kinematics

3.1 INTRODUCTION

Material removal by grinding occurs mainly by a chip formation process, similar to that of other machining methods such as turning or milling, but on a much finer scale. While the cutting-tool geometry and its interaction with the workpiece is well defined for most machining processes, the situation for grinding is not readily discernible. A grinding wheel has a multitude of geometrically undefined cutting points (tools) which are irregularly distributed on its working surface and which are presented to the workpiece at random orientations and positions. Consequently, there is significant variation in the cutting geometry from point to point.

In spite of these complexities, the past 70 years have seen many attempts to analyze chip geometry [1,2], usually in terms of what occurs at a 'typical' or 'average' cutting point rather than at each separate cutting point. Some of these analyses also attempt to describe the point-to-point variability in cutting geometry by using either statistical models or computer simulations to describe how the non-uniform wheel surface interacts with the workpiece.

This chapter presents a mathematical analysis of the cutting geometry during grinding, arising from consideration of the kinematic interactions between the topography of the grains in the wheel surface and the workpiece. Aside from leading to fundamental parameters, such as the depth of cut taken by a cutting point (undeformed chip thickness) and the size of the grinding zone (contact length), it also provides a basis for analyzing the mechanisms of abrasive interactions with the workpiece (Chapter 5), the grinding temperatures (Chapter 6), and the geometry of the ground surface generated (Chapter 7).

3.2 GEOMETRICAL WHEEL–WORKPIECE CONTACT LENGTH

The grinding geometry is illustrated in Fig. 3.1 for straight, external, and internal cylindrical grinding. For straight surface grinding (Fig. 3.1(a)), a wheel of diameter